

High power primary lithium ion microbatteries

James H Pikul¹, Paul V Braun^{1,2} and William P King^{1,2}

¹ Department of Mechanical Science and Engineering, University of Illinois at Urbana – Champaign, 1206 W. Green st., Urbana, IL, USA 61801

² Department of Materials Science and Engineering, University of Illinois at Urbana – Champaign, 1304 W. Green st., Urbana, IL, USA 61801

E-mail: jpikul2@illinois.edu

Abstract. Microbatteries are a critical component for powering autonomous and remote microdevices, but current microbatteries lack the power density and capacity required for high performance use. This paper reports primary microbatteries with high power density and capacity. The microbatteries are based on interdigitated three-dimensional nanoporous bicontinuous electrodes, which enable short ion diffusion lengths and high discharge power. The microbatteries utilize a high capacity manganese oxide cathode and lithium anode to achieve a capacity of up to $29.5 \mu\text{Ah}/\text{cm}^2\mu\text{m}$, which is 10X the average capacity of the highest capacity rechargeable microbatteries reported.

1. Introduction

The capacity and power density of microbatteries directly impact the operation time and performance of the devices they power. The capacity of a battery is dependent on the total volume and capacity of the anode and cathode electrolytic materials, materials that undergo an electrochemical reaction. Thin film microbatteries made by layering films, about $1 - 10 \mu\text{m}$, of cathode, electrolyte, and anode on metal current collectors have high volumetric capacity ($16 - 21 \mu\text{Ah}/\text{cm}^2\mu\text{m}$) [1, 2]. The 2-D nature of thin film batteries gives them poor areal capacity, often making them much larger than the devices they power [3]. Recent research on microbatteries has focused on creating 3D electrodes, so that the areal capacity is high (up to $3,500 \mu\text{Wh}/\text{cm}^2$) and the battery is of similar shape and size to the device it powers [4-7]. The focus on high areal capacity has led to microbatteries with volumetric capacities 5 – 5,000 X lower than conventional lithium ion batteries [8]. The low capacity of microbatteries is due to the fabrication difficulty of packing high volumes of anode and cathode material within 10's of μm spacing and the use of low capacity materials.

Microbatteries also suffer from low power density, typically below $3.5 \mu\text{W}/\text{cm}^2\mu\text{m}$ [4-7]. Specifically engineered structures with short ion transport lengths and highly conductive electrodes are required to achieve high power density [9]. Only recent microbattery work with an interdigitated 3D bicontinuous nanoporous architecture has demonstrated power densities up to $7.4 \text{mW}/\text{cm}^2\mu\text{m}$, which was 2,000 X the power density of other 3D microbatteries and similar to supercapacitors [8].

Here we report primary, single discharge, microbatteries that use high capacity manganese oxide conversion compounds to achieve high power and high energy density. The microbatteries are based on interdigitated 3D nanoporous bicontinuous electrodes, which enable short ion diffusion lengths and



high discharge power with a large volume of electrolytic material. The microbatteries can be pulsed at 20 mA/mm^3 current densities for over 100 times to deliver high on-demand power. The microbatteries utilize primary battery chemistry to achieve a capacity of up to $29.5 \text{ } \mu\text{Ah/cm}^2\mu\text{m}$, 10X the average capacity of the highest capacity rechargeable microbatteries previously reported by us [8].

Figure 1 shows the microbattery design. The porous electrodes are interdigitated with alternating anode and cathode. The electrodes are composites composed of a highly porous bicontinuous nickel current collector conformally coated with lithium or manganese oxide, for the anode and cathode. The microbattery architecture offers short ion diffusion lengths in the electrolytic material and electrolyte and highly conductive continuous electron pathways in the nickel scaffold to reduce transport resistances and achieve high power density [8-10]. The high capacity primary chemistry, low cut-off voltage, and large volume fraction of electrolytic material enables high volumetric capacity.

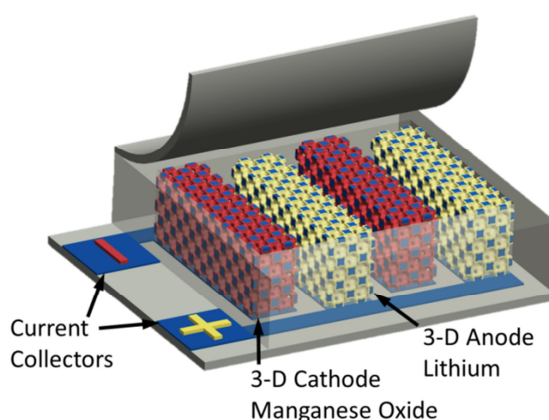


Figure 1. Microbattery design. The nanoporous microbattery electrodes consists of an electrolytically active layer (red and yellow) coated on an electrically conductive bicontinuous nickel scaffold (blue). The nickel scaffold acts the current collector attached to an outside circuit. A manganese oxide is used as the cathode (red), and lithium as the anode (yellow).

2. Methods

The microbatteries were fabricated by electrodeposition electrolytic material onto porous metal scaffolds. Electrodeposition allowed for precise, conformal deposition of the active materials so that a large volume of active material could be deposited without shorting the microbattery. Figure 2 shows the microbattery fabrication, which followed a similar procedure developed by us in [8]. An opal structure was first self-assembled onto a glass substrate with interdigitated gold templates. The interdigitated templates had 5 mm long and $5 \text{ } \mu\text{m}$ wide parallel rectangles, called fingers, connected to two perpendicular 4 mm wide contacts. The glass slide with interdigitated gold templates was then cut into multiple samples, piranha cleaned for ten minutes, immersed in Millipore water with 2.2 % by weight 3-mercapto-1-propanesulfonic acid, sodium salt for 3 hours and rinsed. The PS opal was self-assembled onto the substrates by placing them vertically in a colloid solution of 500 nm in diameter PS spheres set on a hot plat at $55 \text{ } ^\circ\text{C}$, covered, and left for 24 hours. The substrates were then sintered at $96 \text{ } ^\circ\text{C}$ for 10 hours to increase the interconnect size between the PS spheres. A larger interconnect size allowed for a thicker active material coating. The porous, bicontinuous nickel current collectors were fabricated by electrodepositing nickel through the PS opal at a constant -2.0 volts versus a nickel reference electrode for 18 minutes in commercial plating solution. The PS was removed by immersing the substrates in two toluene baths for 3 hours each followed by a toluene and tetrahydrofuran rinse.

Voltage controlled, pulsed electrodeposition was used to deposit the lithium and manganese oxide active material to ensure conformal coating throughout the 3D structure. The nickel scaffold was first primed for manganese deposition by a applying a 1.2 and -0.5 pulsed voltage to the nickel electrode

for 0.1 and 3.0 seconds and 50 cycles with a Ag/AgCl reference and steel counter electrode in a 0.1 M manganese acetate and 0.1 M sodium sulfate solution. Manganese oxide was deposited on to the cathode nickel scaffold using a three electrode deposition, where a sheet of platinum 3 cm² was the working electrode, Ag/AgCl was the reference electrode, and the microbattery substrate attached to a 25 cm² steel sheet was the counter electrode. A 1.3, 1.1, and 0 volts pulsed voltage signal was applied to the platinum for 0.1, 0.5, and 10 seconds for 275 cycles. Manganese oxide was plated onto the substrate during the application of 0 volts to the platinum electrode. The pulsed and exponentially decreasing current applied to the nickel current collector allowed for a highly conformal and thick deposition, which is critical for achieving a large volume fraction. A 1 mm thick polyethylene mask with a 0.5 to 4 mm² through hole and acrylic monomer adhesive was pressed on to a 110 °C pre-heated microbattery substrate and then cooled to room temperature. Figure 3 shows scanning electron microscopy images of the microbattery. Figure 3a is a top-down view of the interdigitated electrodes with a representation of the area covered by the mask. Figure 3b shows a cross-section of the electrodes, before lithium deposition. The electrodes are 15 μm tall and 30 μm wide with a 40 μm period. The nickel current collector has 500 nm pores.

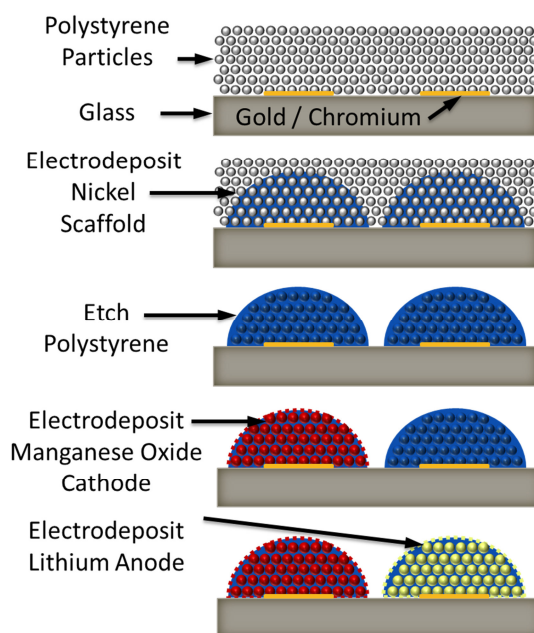


Figure 2. Schematic of the fabrication process where the nickel scaffold defines the battery architecture and the active materials are electrodeposited onto the nickel scaffold for precise integration of the electrodes on a single substrate. The nickel scaffold is formed by electrodepositing nickel through a polystyrene scaffold on glass with gold interdigitated electrodes.

The microbattery substrate was moved to an Argon glovebox and lithium was deposited on to the anode nickel scaffold using a pulsed voltage of -0.5 for 4 seconds and 0 amp off current for 6 seconds versus lithium metal in 1:1 ethylene carbonate (EC) and dimethyl carbonate (DMC) with 1 M LiClO₄ for 40 cycles. 1:1 EC:DMC with 1 M LiClO₄ liquid electrolyte was then dropped in to the mask opening and the microbattery cell was tested by galvanostatically discharging the cells to 0.5 volts at various current densities and pulsed discharges.

The energy and power density of the microbattery cells were obtained by measuring the voltage and current during the cell discharge, calculating the total energy and power, and normalizing the energy and power to the volume of the microbattery cell, which includes the total volume occupied by the electrodes (anode, cathode, Ni current collector, and electrolyte in the porous 3D electrode) and the

electrolyte in the separation between the electrodes. The volume was calculated by multiplying the height of the electrodes by the total area of the cell not covered by the mask.

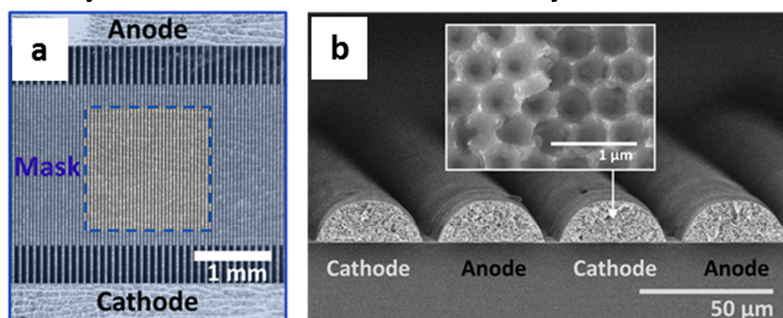


Figure 3. (a) A top-down SEM image of the interdigitated electrodes with the anode electrodes connecting at the top, cathode electrodes connecting at the bottom, and the interdigitated anode and cathode in the middle. A polyethylene mask, illustrated in blue, is placed on the electrodes to control the active discharge area. (b) Cross-section SEM of the electrodes with a close up of the cathode.

3. Results and Discussion

Figure 4a shows the discharge curve for a primary microbattery. The total capacity stored was $29.5 \mu\text{Ah}/\text{cm}^2\mu\text{m}$. The discharge voltage range is between 3.2 and 0.5 volts, with most of the capacity stored between 1.5 and 0.5 volts. The 0.5 to 1.5 voltage plateau is similar to the plateau seen in the first 400 mAh/g capacity of other manganese oxide conversion anodes [11-14]. Manganese oxides that undergo conversion reactions have been studied as anodes for lithium ion batteries due to their high capacity and low voltage. Here we use the manganese oxide as a cathode because of its high capacity relative to conventional cathodes, typically 100 – 200 mAh/g [15]. Conventional cathodes have an advantage due to their high voltage versus lithium, $\sim 2 - 4$ volts, despite their low capacity. The high voltage output improves energy density and also interfaces well with electronics since most electronics require greater than 1.8 volts to operate. However, recent work in low power and energy harvester electronics has seen the development of boost converters that operate with $>90\%$ efficiency and can up convert from 0.3 to 5.0 volts input to a constant 1.8 to 5.5 volts output, like the Texas Instruments tps61200. These technologies allow batteries to be efficiently discharged to lower voltages and opens the possibility of using high capacity anode materials as cathodes in primary batteries. The capacity of anode materials can be up to 4,200 mAh/g for silicon and 1,300 mAh/g during the first discharge of conversion manganese oxides [11-13, 16]. Lithium is used as the anode because of its high capacity and low, constant voltage relative to the cathode.

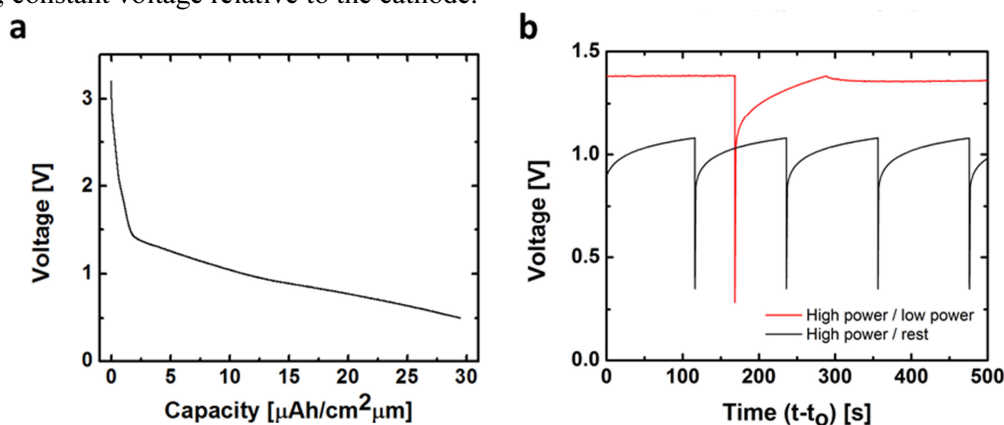


Figure 4. (a) A microbattery discharge curve. Most of the energy is stored between 1.5 and 0.5 volts. (b) Sections of pulsed discharge curves for a microbattery. The red curve shows the battery voltage after 50% discharge during a high current $1950 \mu\text{A}/\text{cm}^2\mu\text{m}$ pulse for 50 ms, followed by a 2 minute rest

and 15 minute low power discharge. The black curve shows the battery voltage after 85% discharge during a $970 \mu\text{A}/\text{cm}^2\mu\text{m}$ pulse for 50 ms, followed by a 2 minute rest.

The microbattery cells can deliver a high power density of $5,500 \mu\text{W}/\text{cm}^2\mu\text{m}$, which is close to the $7,400 \mu\text{W}/\text{cm}^2\mu\text{m}$ highest power reported for microbatteries and superior to most supercapacitors [8]. The microbatteries can alternate between a high power pulsed discharge and a low power sleep discharge, which is critical for applications requiring wireless communication and device actuation. Figure 4b shows discharge profiles of a microbattery during various types of pulsed discharges. The microbattery was discharged at $1950 \mu\text{A}/\text{cm}^2\mu\text{m}$ current for 120 pulses and $970 \mu\text{A}/\text{cm}^2\mu\text{m}$ for 180 pulses. The microbattery was discharged to 0 volts during the high power pulses, similar to capacitors, to maximize the power performance. The microbattery voltage returned to ~75% of its voltage before the high rate discharge within 1 second of rest. The microbatteries can be repeatedly discharged at high power with no noticeable performance degradation.

4. Conclusion

High power and high capacity primary microbatteries have been fabricated by electrodepositing high capacity electrolytic materials on an interdigitated 3D nanoporous bicontinuous architecture. The high capacity manganese oxide cathode demonstrated a new way to use what are typically considered anode materials to dramatically improve the capacity of micro energy storage technologies. The high power pulsed operation of the microbatteries can improve the performance and lifetime of devices that rely heavily on actuation or wireless communication. High capacity and high power density primary microbatteries could increase the capacity of micro power sources by 20X and improve the power performance by 1,000X by replacing the rechargeable battery and energy harvester typically used to power microsystems, enabling smaller power sources, faster computation, stronger actuation, and longer data transmission distances for short to medium lifetime devices.

References

- [1] Drews J, Fehrmann G, Staub R and Wolf R, *J. Power Sources*, **97–98**, 747-9
- [2] Lee Y-G, Kim J, Kim S and Kim K M, *J. Power Sources*, **195**, 3715-9
- [3] Arthur T S, Bates D J, Cirigliano N, Johnson D C, Malati P, Mosby J M, Perre E, Rawls M T, Prieto A L and Dunn B, *MRS Bulletin*, **36**, 523-31
- [4] Chamran F, Yeh Y, Min H S, Dunn B and Kim C J, *J. Microelectromech. Syst.*, **16**, 844-52
- [5] Min H S, Park B Y, Taherabadi L, Wang C L, Yeh Y, Zaouk R, Madou M J and Dunn B, *J. Power Sources*, **178**, 795-800
- [6] Nathan M, Golodnitsky D, Yufit V, Strauss E, Ripenbein T, Shechtman I, Menkin S and Peled E, *J. Microelectromech. Syst.*, **14**, 879-85
- [7] Kotobuki M, Suzuki Y, Munakata H, Kanamura K, Sato Y, Yamamoto K and Yoshida T, *Electrochim. Acta*, **56**, 1023-9
- [8] Pikul J H, Gang Zhang H, Cho J, Braun P V and King W P, *Nat. Commun.*, **4**, 1732
- [9] Braun P V, Cho J, Pikul J H, King W P and Zhang H, *Curr. Opin. Solid State Mater. Sci.*, **16**, 186-98
- [10] Zhang H, Yu X and Braun P V, *Nat. Nanotechnol.*, **6**, 277-81
- [11] Deng Y, Li Z, Shi Z, Xu H, Peng F and Chen G, *RSC Advances*, **2**, 4645-7
- [12] Gao J, Lowe M A and Abruña H D, *Chem. Mater.*, **23**, 3223-7
- [13] Chang L, Mai L, Xu X, An Q, Zhao Y, Wang D and Feng X, *RSC Advances*, **3**, 1947-52
- [14] Wang H, Cui L-F, Yang Y, Sanchez Casalongue H, Robinson J T, Liang Y, Cui Y and Dai H, *J. Am. Chem. Soc.*, **132**, 13978-80
- [15] Goodenough J B and Kim Y, *Chem. Mater.*, **22**, 587-603
- [16] Boukamp B A, Lesh G C and Huggins R A, *J. Electrochem. Soc.*, **128**, 725-9